Ionics
https://doi.org/10.1007/s11581-024-06052-9

RESEARCH

Polyether (polyethylene oxide) derived carbon electrode material and polymer electrolyte for supercapacitor and dye-sensitized solar cell

Sehrish Nazir[1] · Pramod K. Singh[1] · Neelam Rawat[2] · Amrita Jain[3] · Monika Michalska[4] · M. Z. A. Yahya[5] · S. N. F. Yusuf[6] · Markus Diantoro[7]

Received: 22 September 2024 / Revised: 6 November 2024 / Accepted: 27 December 2024
© The Author(s), under exclusive licence to Springer-Verlag GmbH Germany, part of Springer Nature 2025

Abstract

This study investigates the development and performance analysis of a supercapacitor using activated carbon synthesized from polyethylene oxide (PEO) as the electrode material, and a poly(vinylidene fluoride-co-hexafluoropropylene) (PVdF-HFP)-based polymer electrolyte, prepared using a solution-cast technique for dye-sensitized solar cell (DSSC) application. This paper deals with polyether-based electrochemical devices, where electrode material is developed by polyethylene oxide (PEO), while an electrolyte is prepared using PVdF-HFP. Detailed electrical and photoelectrochemical studies were carried out using various characterization tools, and the results are discussed in detail. Sandwich structure supercapacitors and DSSCs are developed using maximum conducting polymer electrolyte that has an ionic conductivity of (8.3×10^{-5}) Scm^{-1}, exhibiting a high specific capacitance of 395 Fg^{-1} and DSSC efficiency ranging from 1.6 to 3.5% under 1 sun condition. The findings underscore the capability of PEO-derived carbon and polymer electrolytes in improving the efficiency of energy storage and conversion systems.

Keywords Polyether · Activated carbon · Supercapacitor · Dye-sensitized solar cell

✉ Pramod K. Singh
pramodkumar.singh@sharda.ac.in

[1] Center for Solar-Cells and Renewable Energy (CSRE), Department of Physics, SSBSR, Sharda University, Greater Noida 201310, India

[2] Department of Chemistry, DSB Campus, Kumaun University, Nainital, Uttarakhand 263001, India

[3] Institute of Fundamental Technological Research, Polish Academy of Sciences, Pawinskiego 5 B, 02-106 Warsaw, Poland

[4] Department of Chemistry and Physico-Chemical Processes, Faculty of Materials Science and Technology, VSB-Technical University of Ostrava, 17. Listopadu 2172/15, 708-00 Ostrava-Poruba, Czech Republic

[5] Faculty of Defence Science and Technology, Universiti Pertahanan Nasional Malaysia (UPNM), 57000 Kuala Lumpur, Malaysia

[6] Center for Ionics University of Malaya, Department of Physics, Faculty of Science, University of Malaya, 50603 Kuala Lumpur, Malaysia

[7] Department of Physics, Faculty of Mathematics and Natural Science, Universitas Negeri Malang, Semarang 5, Malang 65145, Indonesia

Introduction

The challenges that come with the depletion of fossil fuels are still prevalent in modern civilizations today, and they include rising fuel prices, a dirty atmosphere, poor environmental conditions, and global warming. One of the main objectives is to solve these issues, which can be done by creating new energy sources and storage technologies [1, 2]. As a result, high specific power and energy storage devices, such as batteries, supercapacitors, and dye-sensitized solar cells are desperately needed.

Supercapacitors, also known as ultra-capacitors or electric double-layer capacitors, are energy storage devices that have high efficiency and low internal resistance since they do not heat up as much as batteries do when short-circuited which makes them safer to use and more useful for applications that require frequent storage [3]. They can deliver a greater amount of energy compared to batteries because of their energy storage method. The process entails a straightforward division of charges between the electrode and electrolyte. A supercapacitor consists of two electrodes, an electrolyte, and a separator. The separator provides

Published online: 06 January 2025

electrical isolation between the two electrodes. Electrode materials are the essential element of every supercapacitor. Supercapacitors possess distinct advantages as compared to other energy storage devices [4]. These include a lengthy cycle life, adaptable packaging, high power output, a wide temperature range, lightweight construction, and little maintenance requirements [5]. Supercapacitors are most suitable for applications that require short load cycles and great dependability. These include power recovery sources such as forklifts, load cranes, electric cars, and energy quality improvement. Potential applications of supercapacitors include fuel-cell buses/cars and light-emission hybrid automobiles [6]. Supercapacitors provide unique characteristics that make them suitable for use as temporary energy storage devices in conjunction with batteries or fuel cells. This combination allows for increased power efficiency and the ability to capture and store energy from braking systems.

Supercapacitors are often categorized into three distinct categories, which are determined by the method used for storing energy. The first type of capacitor is the electrical double-layer capacitor (EDLC). In this case, the capacitance is mostly determined by the electrode surface area that is accessible to the electrolyte ions, which store the pure electrostatic charge at the interface between the electrode and the electrolyte [7]. Furthermore, within this category, the pseudocapacitor exhibits a rapid and reversible faradic process as a result of electroactive species [8]. The hybrid capacitor represents the third group. It exhibits a combination of both EDLC and pseudocapacitor features [9]. The choice of electrode material in supercapacitors is crucial since it directly influences the electrical characteristics. The surface properties of the electrode material have a significant impact on the capacitance of the cell due to the fact that the storage of double-layer charge occurs mostly at the surface. Supercapacitors have several disadvantages, including poor specific energy, low voltage per unit cell, and rapid self-discharge [10]. One highly innovative and intensive method to address the challenge of low specific energy is the discovery of novel electrode materials for supercapacitors. Currently, the most widely used electrode materials include carbon-based materials, metal oxides/sulfides, and conducting polymers [11]. Carbon materials have been used in the early phase of supercapacitor production due to their distinctive characteristics, including a significant surface area, excellent conductivity, and strong stability. Metal oxides and sulfides are appealing choices for electrode materials due to their high specific capacitance and low resistance, enabling the creation of supercapacitors with high energy and power. In the case of conducting polymers, the reduction–oxidation process is employed to store and release charge. Figure 1 displays a schematic representation and classification of various types of supercapacitors.

Supercapacitors and dye-sensitized solar cells (DSSCs) have gained considerable interest for their potential use in renewable energy systems, portable electronics, and electric cars, as they offer sustainable and efficient energy storage and conversion technologies [12]. Supercapacitors have the ability to charge and discharge quickly, have a high amount of power per unit volume, and can last for a long time. On the other hand, DSSCs are a cost-effective option for traditional silicon-based solar cells [13]. They have adjustable optical properties and are easy to manufacture. The effectiveness of these systems relies heavily on the electrode materials utilized, specifically the carbon-based materials

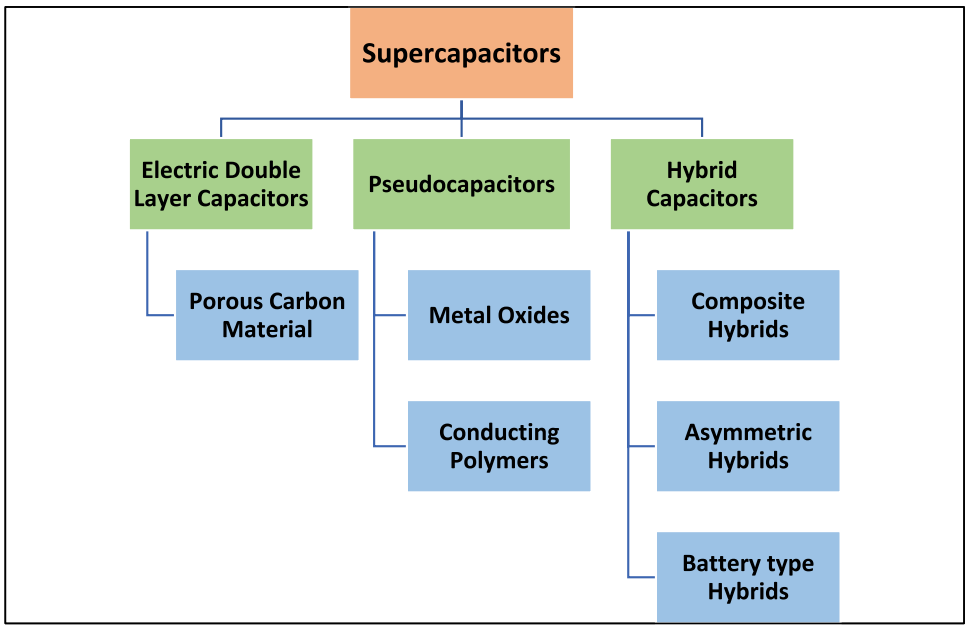

Fig. 1 Schematic representation of various types of supercapacitors

that are essential for energy storage and charge transfer mechanisms.

Porous carbonaceous materials are conventionally manufactured through physical activation, chemical activation, or a mix of both methods [14]. Prior to this, very porous carbons were generated by employing KOH as a chemical activating agent, utilizing precursors such as linear polymers, carbon nanotubes, and graphene oxide. The microporous solid precursors with enhanced properties for carbonaceous materials, metal–organic frameworks (MOFs), porous aromatic frameworks (PAFs), conjugated microporous polymers (CMPs), and hypercrosslinked polymers (HCPs) [15].

The performance and application of energy storage devices heavily rely on the electrode or electrode materials used in them [16–18]. Porous carbon (PC) materials find use in several fields such as water purification [19], chromatography [20], gas separation [21], catalyst support [22], energy storage [23, 24], and conversion [25]. Consequently, PC is widely recognized as the optimal and cost-effective option for enhancing the efficiency of these devices [26]. PC material is a carbon-based substance that contains pores. A typical carbon skeleton seen in PC-based materials consists of a randomly arranged network of graphene layers or aromatic sheets with defects. PC is defined and distinguished by its pore size, with pores larger than 50 nm referred to as macropores, pores smaller than 2 nm referred to as micropores, and pores ranging from 2 to 50 nm referred to as mesopores [27]. The literature has already documented that PC possesses remarkable attributes, including elevated electrical conductivity [28], surface area, chemical stability, and a substantial pore volume [29]. Given these characteristics, it is appropriate for utilization as electrode material. Nevertheless, it is imperative to obtain high-quality carbon from environmentally sustainable sources. In recent times, numerous research efforts have attempted to produce large quantities of PC from waste materials such as polyvinyl chloride [30], corn starch [31], banana peels [32], orange peels [33], and others. These sources provide a cost-effective and eco-friendly means of acquiring high-quality electrode materials. In addition, individuals have utilized commercial high-quality PC-based electrodes for a range of purposes. Nevertheless, their usage incurs significant expenses. PC for electrode application in SC is being developed using standard-grade PC and natural, environmentally friendly carbon precursors, such as peanut shells [34], coconut shells [35], palm shells [36], coal [37], rice husk [38], leaves [39], and polymers [40]. Organic polymers are the optimal option for synthesising PC because of their regulated composition and structure, consistent qualities, high carbon content, low ash content, and high purity. Consequently, several organic polymers, including carbazole-terephthalaldehyde-based copolymer, poly (para-phenylenediamine), polyvinyl chloride, polystyrene, polypyrrole, and chitosan, have been employed in the production of different types of PC for supercapacitors (SC) [41]. Polyether-based electrolytes are well-known materials used in DSSCs. DSSC comprises three parts, that is, working electrode, redox couple doped polyether electrolyte and counter electrode. Regarding the electrolyte component, high conductivity is a well-known characteristic correlated with current density (J_{SC}). In the development of highly conductive polymer electrolytes, polyethers are pivotal, with doping in the polymer being important. In the present case, we are attempting to incorporate low viscosity ionic liquids (ILs) into a polyether-based electrolyte.

Polyethers are polymers composed of monomers connected by ether bonds, which are formed by bonding two carbon atoms to an oxygen atom [42]. A diverse range of polyethers is manufactured, encompassing elastomers and engineering plastics. The structures of the compounds exhibit substantial variation, although they always maintain the $C-O-C$ linkage. Polyethers can exist in either aliphatic or aromatic forms [43]. Polyethylene oxide (PEO) [44], polypropylene oxide (PPO) [45], and polytetrahydrofuran are examples of aliphatic polyethers that possess flexibility and a relatively low degree of crystallinity. They are occasionally referred to as polyether glycols due to the presence of hydroxyl groups at the extremities of their chains. Polyethylene glycol (PEG) and polypropylene glycol are synonyms for the initial two components. Base-catalyzed ring-opening polymerization is employed for ethylene and propylene oxides (POs), whilst acid catalysis is utilized for tetrahydrofuran. The viscosity of these polyethers varies from highly viscous liquids to solid waxes, depending on their molecular weight. Polyurethane manufacturing dominates the market for all three materials. Other applications include lubricants, hydraulic fluids, and surfactants [46].

This work discusses the use of activated carbon electrode material obtained from polyether, specifically poly(ethylene oxide) (PEO), for the purpose of supercapacitors. In this study, a supercapacitor was successfully fabricated by using porous carbon derived from PEO [47] and electrolyte–PVDF-HFP and ionic liquid-based polymer electrolyte which was placed between the electrodes. Also, DSSCs were fabricated using the same polymer electrolyte.

Experimental section

Materials used

PEO was used as a precursor to synthesize carbon material already reported by our group [47]. Other chemicals such as H_2SO_4 as an activating agent and HCl for washing were also used. The materials used for the synthesis of polymer electrolyte films are poly(vinylidene fluoride-co-hexafluoropropylene) (PVDF-HFP) as host polymer, sodium thiocyanate

(NaSCN) as ion-source salt, acetone as solvent, and ionic liquid. PVDF-HFP was purchased from Sigma Aldrich (USA), having a molecular weight (Mw) of $4 \times 10^5 gmol^{-1}$. NaSCN of Mw 81.07g mol^{-1} was purchased from Central Drug House, New Delhi (India). The ionic liquid was also purchased from Central Drug House, New Delhi (India). The current collector, i.e., graphite sheet, was purchased from Nickunj Eximp Entp Pvt Ltd, Mumbai.

Synthesis of carbon

The activated porous carbon was prepared using the pyrolysis method. The sample was made by chemically activating it with H_2SO_4 as the activating agent, following the pre-carbonization treatment of the PEO polymer [47]. In order to obtain activated porous carbon, PEO was combined with a concentrated H_2SO_4 solution as an activating agent for a duration of 6–8 h. The combination was subsequently subjected to carbonization in a tube furnace under an inert gas atmosphere, with a heating rate of 5 °C per minute, until reaching a temperature of 800 °C. The mixture was then held at this temperature for 30 min. The sample was returned to the ambient environment using the same temperature rate of 5 °C per minute. The carbon material was prepared and cleansed using HCl then rinsed with double distilled water using a vacuum filtration device. Subsequently, the carbon sample was placed in a vacuum oven and subjected to a temperature of 90 °C in order to remove any moisture. The activated porous carbon obtained from PEO activated with H_2SO_4 was designated as A-PC (activated porous carbon).

Synthesis of polymer electrolyte

Various polymer electrolyte films were developed using the solution-cast process. The appropriate quantities of PVdF-HFP (with a molecular weight of $(4 \times 10^5$g $mol^{-1})$ are dissolved in a commonly used solvent, acetone. We added a predetermined quantity of NaSCN to the solution and stirred it for around 10 h until we achieved a thick, clear solution. Therefore, the PVdF-HFP and sodium thiocyanate (NaSCN) solution was subsequently mixed with varying quantities of IL (x wt% of IL, with x being varied) and stirred overnight to achieve homogeneous solutions. The diverse solutions were subsequently transferred into different Petri dishes and left at room temperature overnight to eliminate all the solvent molecules.

Fabrication of supercapacitor

In order to develop a supercapacitor, a mixture was made using activated-carbon material, acetylene black, and PVDF-HFP as a binder (Fig. 2). A solution was prepared by dissolving 10 wt% of PVDF-HFP in acetone using a magnetic stirrer for a duration of 3–4 h. Subsequently, a mixture of 80 wt% activated-carbon material and 10 wt% acetylene black was ground using a mortar and pestle. Then, a binder solution consisting of PVDF-HFP was added drop by drop to the mixture to form a slurry. Finally, a slurry with a mass of approximately 1 mg was applied to each graphite sheet, which serves as the current collector, covering an area of 1×1 cm^2. The resulting electrodes were then placed in a

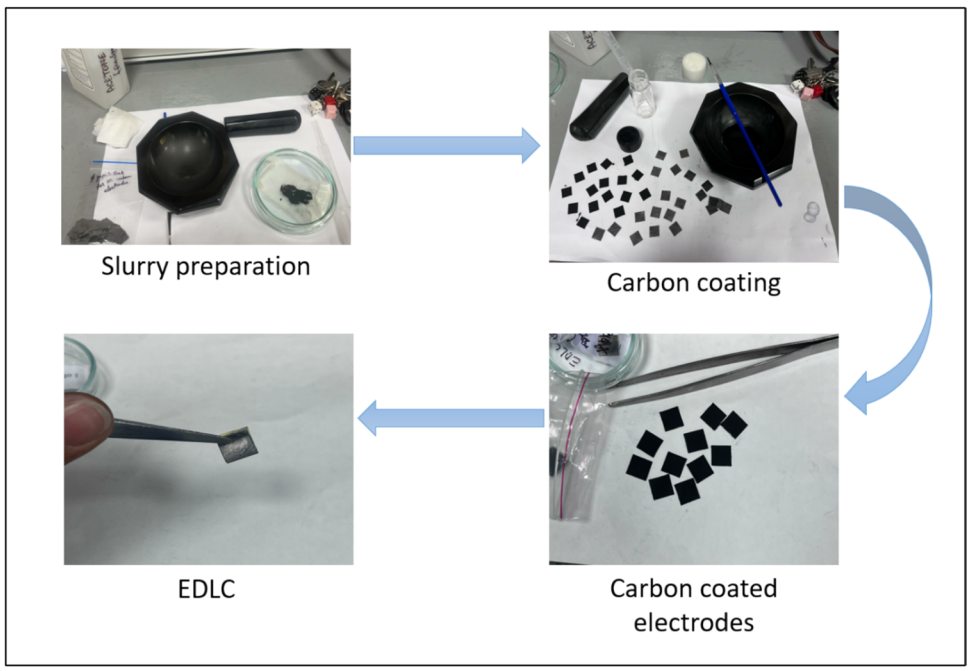

Fig. 2 Schematic diagram of the fabrication of supercapacitor

vacuum oven and subjected to vacuum drying at a temperature of 80 °C for the duration of the night.

The supercapacitor was developed by inserting the optimized ionic liquid-incorporated PVdF-HFP conducting solid polymer electrolyte (with conductivity 8.3×10^{-5} Scm^{-1}) layer between two identical activated-carbon electrodes (graphite sheets covered with activated carbon). Subsequently, the assembled supercapacitor cell was placed in a sample holder to enable additional electrochemical analysis.

Fabrication of dye-sensitized solar cell

The development of dye-sensitized solar cells (DSSCs) starts with the preparation of the photoanode. This involves cleaning a transparent conducting oxide (TCO) glass substrate, that is, fluorine-doped tin oxide (FTO), and applying a mesoporous layer of titanium dioxide (TiO_2) nanoparticles onto it. This can be achieved through methods like doctor blading. Subsequently, the layer is sintered at high temperatures (450–500 °C) in order to improve electron transport and binding. The substrate coated with TiO_2 is submerged in a solution containing dye, which enables the dye molecules to stick to the surface and create a single layer that absorbs light. Simultaneously, the counter electrode is typically an FTO glass that has been coated with a catalyst such as platinum. This is achieved by undergoing deposition and sintering procedures. The photoanode and counter electrode are aligned in a face-to-face configuration, separated by a space between them to ensure a specific distance between them. This gap is then filled with an electrolyte solution that contains an iodide/triiodide redox couple (Fig. 3). The cell is tightly sealed to prevent any electrolyte loss. The DSSC is thereafter subjected to testing using simulated sunlight to assess its photovoltaic performance, specifically its efficiency and stability. DSSCs offer a promising alternative to conventional solar cells due to their simple fabrication procedure that utilizes inexpensive materials and basic procedures.

Results and discussion

Supercapacitor performance

Low-frequency impedance spectroscopy (LIS)

To measure the specific capacitance (C) of the fabricated supercapacitor, we have carried out low-frequency impedance spectroscopy (LIS) using the CH Instrument Electrochemical Workstation (model 604D, USA). The recorded

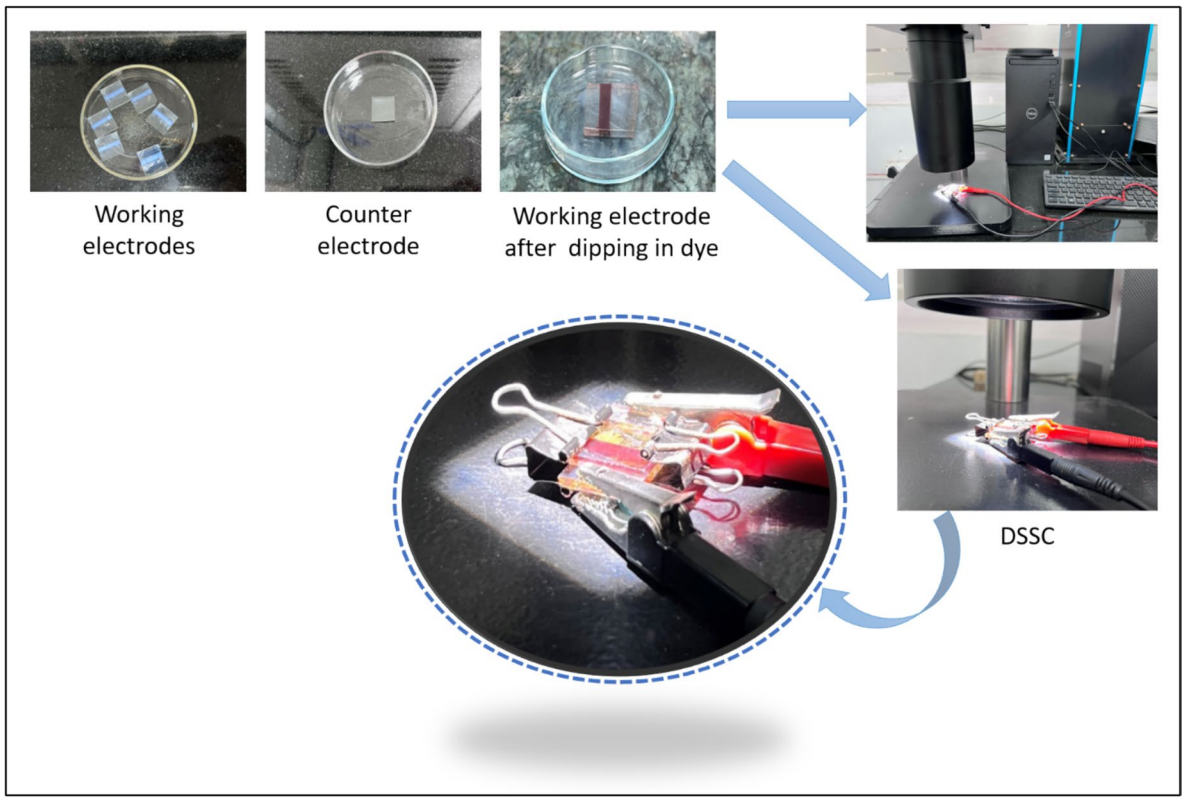

Fig. 3 Schematic diagram of the fabrication of DSSC using a solar simulator

plot (low-frequency impedance spectroscopy plot) shown in Fig. 4 reveals valuable information regarding the electrochemical characteristics of the supercapacitor we fabricated. The supercapacitor was developed using PEO-based activated carbon material and a polymer electrolyte consisting of PVdF-HFP, NaSCN, and tributylmethylphosphonium iodide.

The Nyquist plot in Fig. 4 displays the real component of impedance (Z', represented on the x-axis) in relation to the imaginary component of impedance (Z'', represented on the y-axis).

LIS was carried out to determine the value of specific capacitance by using the formula :

$$C = -\frac{1}{\omega Z \epsilon} \tag{1}$$

In Eq. (1), "ω" is the angular frequency of the applied alternating current (AC) signal in radians per second (rad/s), and it is related to frequency (f) by the formula,$\omega = 2\pi f$

$$So, C = -\frac{1}{2\pi f Z \epsilon} \tag{2}$$

where f is the frequency of the AC signal in hertz (Hz), and Z'' is the imaginary part of the complex impedance Z.

We obtained the maximum specific capacitance of 692 F g^{-1} using low-frequency data.

The plot starts with a small semicircle at increased frequencies, followed by a linear segment at lower frequencies. The semicircle at the starting point of the plot indicates the combined impact of charge transfer resistance (R_{ct}) and double-layer capacitance (C_{dl}).

The smaller semicircle indicates a low charge transfer resistance, which promotes efficient ion transport at the electrode–electrolyte interface.

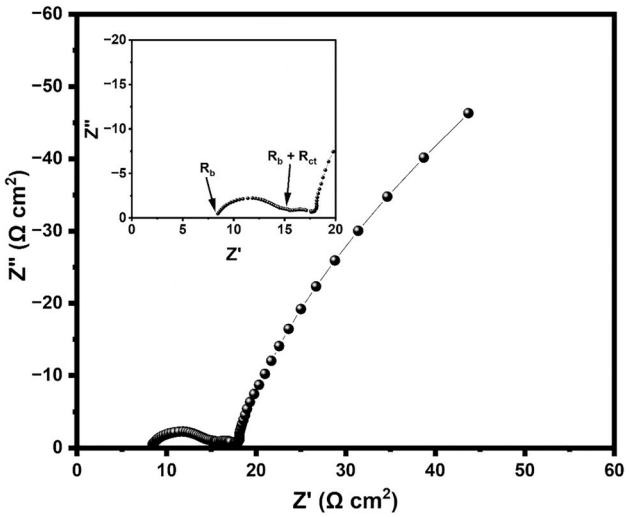

Fig. 4 Low-frequency impedance plot of the supercapacitor cell

As the frequency drops, the plot exhibits a shift to a linear line with an inclination of around 45 degrees, which is a distinctive feature of Warburg impedance and is related to the movement of ions in the electrolyte by diffusion. This signifies the dispersion of ions inside the electrolyte. The steep incline observed at the end of the figure, particularly beyond a value of Z' approximately equal to 20 Ω cm^2, indicates a capacitive response, as anticipated for a supercapacitor. The presence of this vertical line signifies that the device predominantly stores charge via electrostatic (capacitive) mechanisms rather than faradaic (battery-like) processes.

The point where the line intercepts the Z' axis at high frequency indicates the series resistance. The diameter of the semicircle provides a measure of the charge transfer resistance occurring at the interface between the electrode and the electrolyte.

The redox behavior present in the polymer electrolyte could potentially lead to distortions in either the semicircle or the slope of the linear region. The deviations or extra semicircles may be linked to faradaic processes or additional capacitive contributions from the redox-active electrolyte. The presence of a small semicircle at high frequencies suggests very little charge transfer. This shows good conductivity of ions and contact between the electrode and electrolyte.

The value of specific capacitance derived from low-frequency impedance spectroscopy can often be overestimated in comparison to other approaches such as cyclic voltammetry (CV), and it serves as the sole evidence of the supercapacitor device demonstrating capacitive behavior. The actual values obtained from the DC measurement, such as CV, are described next.

Cyclic voltammetry (CV)

To measure the specific capacitance (C) of the fabricated supercapacitor, we have carried out cyclic voltammetry (CV) using the CH Instrument Electrochemical Workstation (model 604D, USA). The cyclic voltammetry (CV) plots illustrate the electrochemical behavior of the fabricated supercapacitor under different conditions. Each plot provides insights into how the device performs under varying voltage windows and scan rates.

The graph shows CV curves at different voltage windows, ranging from 0 to 1 V up to 0 to 2 V as shown in Fig. 5a. The shape of the curves is nearly rectangular, especially at lower voltage windows, which is characteristic of ideal capacitive behavior. At higher voltage windows (close to 2 V), the curve starts to deviate slightly, which could be due to the onset of faradaic reactions or the limits of the electrolyte stability. Figure 5b shows CV curves measured at different scan rates ranging from 5 to 200 mV/s within a voltage window of 0 to 1 V. At lower scan rates, the CV curve is more rectangular, indicating better capacitive behavior. As

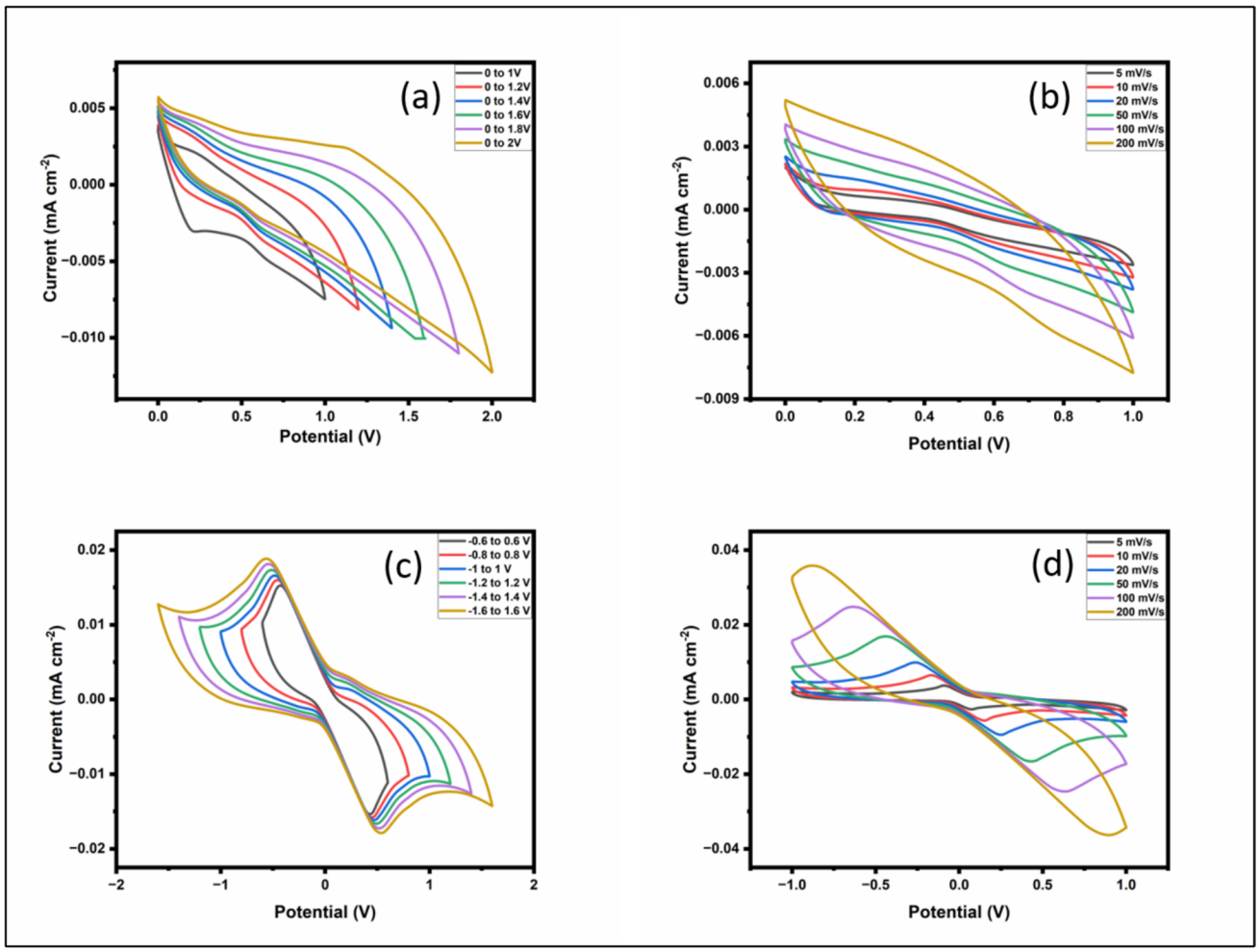

Fig. 5 CV plots at **a** different voltage ranges keeping a scan rate of 50 mVs^{-1}, **b** various scan rates keeping a voltage range of 0 to 1 V, **c** various voltage ranges keeping a scan rate of 50 mVs^{-1}, and **d** various scan rates keeping a voltage range of − 1 to 1 V

the scan rate increases, the curve becomes more distorted, and the peak current increases. This is typical because, at higher scan rates, the ions in the electrolyte do not have sufficient time to fully penetrate the porous structure of the electrode, leading to higher resistive losses. The symmetrical shape of the curves at different scan rates suggests good reversibility of the redox reactions occurring in the system. Figure 5c shows the CV behavior over a negative voltage window, from [− 0.6 to 0.6 V] to [− 1.6 to 1.6 V]. The area under the curve in this plot indicates the charge storage capability in the negative voltage range. The nearly symmetric shape of the curves suggests good reversibility and capacitive behavior. Similar to plot (b), the graph in Fig. 5d shows the CV curves at different scan rates, but in a negative voltage window (− 1 V to 1 V). At lower scan rates, the curve is close to rectangular, indicating efficient charge storage. With increasing scan rates, the curves start to deviate from the rectangular shape, which is a common behavior in supercapacitors, where at higher scan rates, the electrolyte ions cannot keep up with the rapid potential changes. The overlapping curves suggest that the device maintains good capacitive performance over a wide range of scan rates.

The specific capacitance was calculated using cyclic voltammetry (CV), which measures the total charge stored per unit mass of the electrode material by the following equation:

$$C = \frac{i}{s} \tag{3}$$

where "C" represents the specific capacitance, "i" represents the current, and "s" represents the scan rate.

The polyether-based activated-carbon supercapacitor cell has a maximum specific capacitance of 395 Fg^{-1} at a scan rate of 5 mVs^{-1} (Table 1).

Additionally, Table 1 highlights the specific capacitance of the polyether-carbon-based supercapacitor cell at various scan rates within a voltage range of − 1 to 1 V. The voltage range of − 1 to 1 V was selected to thoroughly investigate

Table 1 Specific capacitance of the supercapacitor cell at varied scan rates (voltage range from − 1 to 1 V)

Scan rate (mVs^{-1})	Specific capacitance ($F\ g^{-1}$)
5	395
10	361
20	295
50	209
100	146
200	76

the electrochemical window of the electrolyte and electrode material. Symmetrically extending the voltage range across both positive and negative values facilitates a more thorough comprehension of supercapacitor behavior. In realistic EDLCs, functioning throughout an extensive voltage range (from negative to positive) facilitates the evaluation of the stability of the device and performance under both cathodic and anodic conditions, offering insights into the energy storage mechanism and possible operational constraints. Furthermore, symmetric voltage cycling guarantees that both electrodes equally participate in charge storage and discharge during testing, facilitating an even evaluation of the capacitive performance of the material. In certain electrolyte systems, operating within the complete potential window (e.g., − 1 to 1 V) optimizes capacitance provided the electrolyte remains stable within this range.

The CV plots confirm the capacitive behavior of the fabricated supercapacitor, as indicated by the nearly rectangular shapes of the CV curves. The deviation from the ideal rectangular shape at higher scan rates and larger voltage windows suggests some resistive and faradaic contributions, possibly from the redox-active polymer electrolyte. The symmetry and stability of the CV curves across different voltage windows and scan rates are indicative of good electrochemical performance and reversibility of the supercapacitor.

Performance of dye-sensitized solar cell (DSSC)

JV characteristics of DSSC

We evaluated the performance of the dye-sensitized solar cell (DSSC) using a solar simulator (model SS-F5-3A, produced by Enlitech, Taiwan), located in our laboratory at the Centre for Solar Cell and Renewable Energy (CSRE) at Sharda University. This solar simulator replicates sunlight in controlled settings, enabling precise testing and measurement of DSSC efficiency. The testing procedure includes a comprehensive investigation of the electrical and optical characteristics of DSSC, principally applying specific mathematical equations to quantify metrics including current density, voltage, power conversion efficiency, and fill factor.

$$Fill\ factor, FF = \frac{V_{max} \times J_{max}}{V_{OC} \times J_{SC}} \tag{4}$$

where

"V_{max}" is the maximum voltage the DSSC can produce during operation, taken from the point on the current–voltage (IV) curve where the product of current and voltage is at its highest.

"J_{max}" is the maximum current density (in $mAcm^{-2}$) at V_{max}, where the product of current and voltage reaches its maximum.

"V_{OC}" is the open-circuit voltage, representing the maximum voltage produced by the DSSC without the presence of an external load (that is, when no current flows).

"J_{SC}" is the short-circuit current density, which refers to the current density when the external load resistance is null (that is, the voltage across the cell is zero). It denotes the highest achievable current density when exposed to light.

$$Efficiency, \eta = \frac{V_{OC} \times J_{SC}}{P_{max} \times FF} \tag{5}$$

where

"V_{OC}" and "J_{SC}" are the open-circuit voltage and short-circuit current density, already defined above.

"P_{max}" is the maximum power output of the DSSC.

"FF" is the fill factor, which is constant for a particular system.

Figure 6 illustrates the estimated J-V curve for the developed dye-sensitized solar cells (DSSCs), and Fig. 6b displays the J-V curve for the DSSC where the highest conducting ionic-liquid-doped solid polymer electrolyte was placed between two electrodes.

The efficiency of DSSCs was evaluated using Eqs. (4) and (5) and are presented in Table 2.

The parameters mentioned in Table 2 were calculated using Eqs. (4) and (5). The developed solar cell demonstrates a consistent efficiency of 3.51% under standard solar illumination conditions.

From Fig. 6 and Table 2, it is clear that DSSC developed using salt-based electrolyte shows efficiency of 1.67%, while IL-incorporated polyether-based DSSC shows efficiency up to 3.5% at one sun condition.

Conclusion

This study illustrates the efficient application of activated carbon derived from polyethylene oxide (PEO) as an electrode material and PVdF-HFP-based electrolyte for

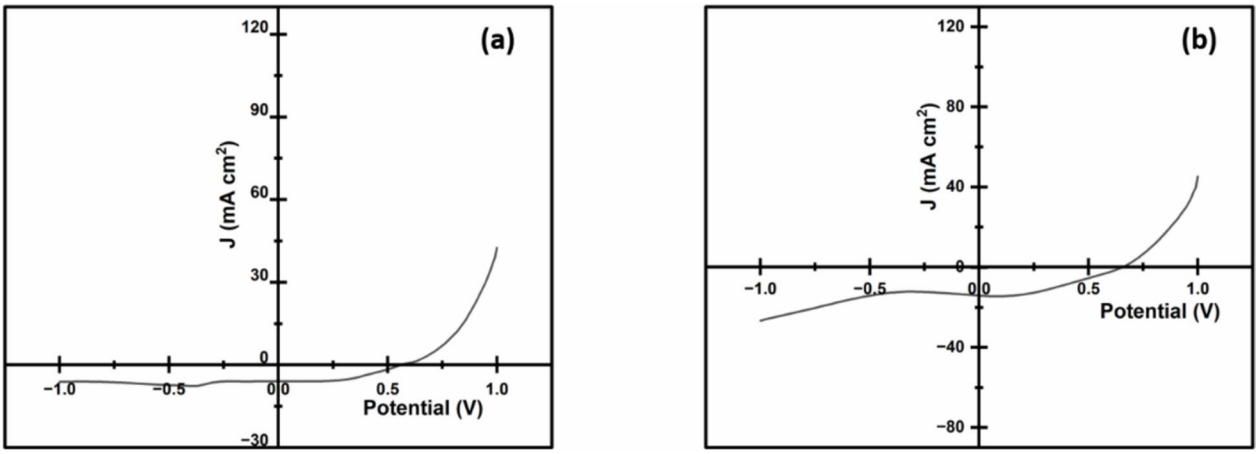

Fig. 6 J-V characteristics of DSSCs with **a** salt and **b** IL under standard solar radiation conditions (one sun)

Table 2 Parameters of dye-sensitized solar cell under standard solar radiation conditions (one sun)

DSSC cell	Area of contact (cm^2)	I_{SC} (mA)	V_{OC} (V)	Fill factor	J_{SC} (mA cm^{-2})	Efficiency (%)
With salt	0.25	1.49	0.56	50.12	5.96	1.67
With IL	0.25	3.52	0.65	38.06	14.08	3.51

supercapacitors and DSSC. Sandwiched supercapacitor using PEO-based activated carbon as electrode material and IL-doped PVdF-HFP-based polymer electrolyte shows high performance, as high as 395 Fg^{-1}, while DSSC using maximum conducting polymer electrolyte shows efficiency as high as 3.51 at 1 sun condition. These high-efficiency values in electrochemical devices certainly indicate that the ionic liquid incorporated polymer may be considered a novel electrolyte for the replacement of liquid electrolytes. Moreover, the high capacitance value also affirms the suitability of PEO-based carbon as electrode material for energy storage applications.

Author contributions Sehrish Nazir, Pramod K. Singh, Neelam Rawat wrote the main manuscript text M. Z. A Yahya, S.N.F. Yusuf , Markus Diantoro prepared the figures and Tables Amrita Jain, Monika Michalska Polished and reviewed the manuscript.

Funding The authors acknowledge the CSTUP (CST/D-1041) and Universitas Negeri Malang under Ministry of Education, Culture, Research and Technology of Indonesia for financial assistance.

References

1. González A, Goikolea E, Barrena JA, Mysyk R (2016) Review on supercapacitors: technologies and materials. Renew Sustain Energy Rev 58:1189–1206. https://doi.org/10.1016/j.rser.2015.12.249
2. Nazir S, Pandey SP, Latif FA, Singh PK (2024) Current scenario and future prospective of ionic-liquid doped polymer electrolyte for energy application. Macromol Symp 413(1):2300035. https://doi.org/10.1002/masy.202300035
3. Jinitha CG, Jeba SV, Sonia S, Ramachandran R (2023) 'Fundamentals of supercapacitors', in *Smart supercapacitors*, Elsevier, pp. 83–100. https://doi.org/10.1016/B978-0-323-90530-5.00014-9.
4. Olabi AG, Abbas Q, Al Makky A, Abdelkareem MA (2022) Supercapacitors as next generation energy storage devices: properties and applications. Energy 248:123617. https://doi.org/10.1016/j.energy.2022.123617
5. Fu W et al (2021) Materials and technologies for multifunctional, flexible or integrated supercapacitors and batteries. Mater Today 48:176–197. https://doi.org/10.1016/j.mattod.2021.01.026
6. Pu Z et al (2021) Regenerative fuel cells: recent progress, challenges, perspectives and their applications for space energy system. Appl Energy 283:116376. https://doi.org/10.1016/j.apenergy.2020.116376
7. Allagui A, Fouda ME (2021) Inverse problem of reconstructing the capacitance of electric double-layer capacitors. Electrochim Acta 390:138848. https://doi.org/10.1016/j.electacta.2021.138848
8. Bhojane P (2022) Recent advances and fundamentals of pseudocapacitors: materials, mechanism, and its understanding. J Energy Storage 45:103654. https://doi.org/10.1016/j.est.2021.103654
9. Sun J, Luo B, Li H (2022) A review on the conventional capacitors, supercapacitors, and emerging hybrid ion capacitors: past, present, and future. Adv Energy Sustain Res 3(6):2100191. https://doi.org/10.1002/aesr.202100191
10. Huang J, Yuan K, Chen Y (2022) Wide voltage aqueous asymmetric supercapacitors: advances, strategies, and challenges. Adv Funct Mater 32(4):2108107. https://doi.org/10.1002/adfm.202108107
11. Kothandam G et al (2023) Recent advances in carbon-based electrodes for energy storage and conversion. Adv Sci 10(18):2301045. https://doi.org/10.1002/advs.202301045

12. Nordin NA et al (2021) Integrating photovoltaic (PV) solar cells and supercapacitors for sustainable energy devices: a review. Energies 14(21):7211. https://doi.org/10.3390/en14217211
13. Mariotti N et al (2020) Recent advances in eco-friendly and cost-effective materials towards sustainable dye-sensitized solar cells. Green Chem 22(21):7168–7218. https://doi.org/10.1039/D0GC01148G
14. Sevilla M, Díez N, Fuertes AB (2021) More sustainable chemical activation strategies for the production of porous carbons. Chemsuschem 14(1):94–117. https://doi.org/10.1002/cssc.202001838
15. Vinodh R et al (2020) A review on porous carbon electrode material derived from hypercross-linked polymers for supercapacitor applications. J Energy Storage 32:101831. https://doi.org/10.1016/j.est.2020.101831
16. Umoren SA, Solomon MM, Saji VS (2022) Polymeric materials in corrosion inhibition: fundamentals and applications. Elsevier, Amsterdam Kidlington, Oxford Cambridge, MA
17. Song Z, Zhou H (2013) Towards sustainable and versatile energy storage devices: an overview of organic electrode materials. Energy Environ Sci 6(8):2280. https://doi.org/10.1039/c3ee40709h
18. Li L et al (2021) Surface and interface engineering of nanoarrays toward advanced electrodes and electrochemical energy storage devices. Adv Mater 33(13):2004959. https://doi.org/10.1002/adma.202004959
19 Sweetman M et al (2017) Activated carbon, carbon nanotubes and graphene: materials and composites for advanced water purification. C 3(2):18. https://doi.org/10.3390/c3020018
20. Knox JH, Kaur B, Millward GR (1986) Structure and performance of porous graphitic carbon in liquid chromatography. J Chromatogr A 352:3–25. https://doi.org/10.1016/S0021-9673(01)83368-9
21. Zhang W, Liu D, Guo X, Huang H, Zhong C (2018) Fabrication of mixed-matrix membranes with MOF-derived porous carbon for CO_2 separation. AIChE J 64(9):3400–3409. https://doi.org/10.1002/aic.16187
22. De S, Balu AM, van der Waal JC, Luque R (2015) Biomass-derived porous carbon materials: synthesis and catalytic applications. ChemCatChem 7(11):1608–1629. https://doi.org/10.1002/cctc.201500081
23. Khan S et al (2022) Synthetic methodologies and energy storage/conversion applications of porous carbon nanosheets: a systematic review. Energy fuels 36(7):3420–3442. https://doi.org/10.1021/acs.energyfuels.2c00077
24. Saeed M et al (2024) 'Potential development of porous carbon composites generated from the biomass for energy storage applications', Chem – Asian J p. e202400394 https://doi.org/10.1002/asia.202400394.
25. Li Y, Fu Z, Su B (2012) Hierarchically structured porous materials for energy conversion and storage. Adv Funct Mater 22(22):4634–4667. https://doi.org/10.1002/adfm.201200591
26. Nair GB, Swart HC, Dhoble SJ (2020) A review on the advancements in phosphor-converted light emitting diodes (pc-LEDs): phosphor synthesis, device fabrication and characterization. Prog Mater Sci 109:100622. https://doi.org/10.1016/j.pmatsci.2019.100622
27. Lawrence M, Jiang Y (2017) 'Porosity, pore size distribution, micro-structure', in Bio-aggregates based building materials, S. Amziane and F. Collet, Eds., in RILEM State-of-the-Art Reports, Dordrecht: Springer Netherlands, 23:39–71. https://doi.org/10.1007/978-94-024-1031-0_2.
28. Lu S, Jin M, Zhang Y, Niu Y, Gao J, Li CM (2018) Chemically exfoliating biomass into a graphene-like porous active carbon with rational pore structure, good conductivity, and large surface area for high-performance supercapacitors. Adv Energy Mater 8(11):1702545. https://doi.org/10.1002/aenm.201702545
29. Leng L et al (2021) An overview on engineering the surface area and porosity of biochar. Sci Total Environ 763:144204. https://doi.org/10.1016/j.scitotenv.2020.144204
30. Hussin F, Aroua MK, Kassim MA, Ali UFMd (2021) Transforming plastic waste into porous carbon for capturing carbon dioxide: a review. Energies 14(24):8421. https://doi.org/10.3390/en14248421
31. Gao R, Guo W, Zhang Y, Zhang Q, Li Y, Wang J (2024) Enhancement of gelatinization on electrochemical performance of corn starch-based porous carbon as electrode material in supercapacitors. Diam Relat Mater 141:110598. https://doi.org/10.1016/j.diamond.2023.110598
32. Fasakin O et al (2018) Synthesis and characterization of porous carbon derived from activated banana peels with hierarchical porosity for improved electrochemical performance. Electrochim Acta 262:187–196. https://doi.org/10.1016/j.electacta.2018.01.028
33. Xu C, Hu Z, Wang X, Wang C, Huang D, Qian Y (2021) Facile preparation of hierarchical porous carbon from orange peels for high-performance supercapacitor. Int J Electrochem Sci 16(3):210350. https://doi.org/10.20964/2021.03.07
34. Liang K et al (2023) Peanut shell waste derived porous carbon for high-performance supercapacitors. J Energy Storage 70:107947. https://doi.org/10.1016/j.est.2023.107947
35. Fahmi F, Dewayanti NAA, Widiyastuti W, Setyawan H (2020) Preparation of porous graphene-like material from coconut shell charcoals for supercapacitors. Cogent Eng 7(1):1748962. https://doi.org/10.1080/23311916.2020.1748962
36. Li J, Lin Q, Wang Z, Du A, Luo H, Liu Y-Q (2023) Hierarchical porous carbon with high specific surface area and superb capacitance made from palm shells for supercapacitors. Diam Relat Mater 135:109852. https://doi.org/10.1016/j.diamond.2023.109852
37. Gao F, Zang Y, Wang Y, Guan C, Qu J, Wu M (2021) A review of the synthesis of carbon materials for energy storage from biomass and coal/heavy oil waste. New Carbon Mater 36(1):34–48. https://doi.org/10.1016/S1872-5805(21)60003-3
38. Xue B, Wang Z, Zhu Y, Wang X, Xiao R (2021) Sustainable and recyclable synthesis of porous carbon sheets from rice husks for energy storage: a strategy of comprehensive utilization. Ind Crops Prod 170:113724. https://doi.org/10.1016/j.indcrop.2021.113724
39. Cha SM, Nagaraju G, Sekhar SC, Bharat LK, Yu JS (2018) Fallen leaves derived honeycomb-like porous carbon as a metal-free and low-cost counter electrode for dye-sensitized solar cells with excellent tri-iodide reduction. J Colloid Interface Sci 513:843–851. https://doi.org/10.1016/j.jcis.2017.11.080
40. Wang H et al (2020) Polymer-derived heteroatom-doped porous carbon materials. Chem Rev 120(17):9363–9419. https://doi.org/10.1021/acs.chemrev.0c00080
41. Liu X et al (2022) Porous organic polymers for high-performance supercapacitors. Chem Soc Rev 51(8):3181–3225. https://doi.org/10.1039/D2CS00065B
42. Price CC (1974) Polyethers. Acc Chem Res 7(9):294–301. https://doi.org/10.1021/ar50081a003
43. Zhang J et al (2021) A high energy density flexible solid-state supercapacitor based on poly (arylene ether sulfone) copolymers with polyether side chains for Li+ conducting polymer electrolytes. Mater Chem Phys 267:124623. https://doi.org/10.1016/j.matchemphys.2021.124623
44. Hui C-Y, Kan C-W, Chau K-H (2023) A study on poly(ethylene oxide)-based supercapacitors doped with various dopants. Coatings 13(8):1373. https://doi.org/10.3390/coatings13081373
45. Kim S et al (2021) Cross-linked composite gel polymer electrolyte based on an H-shaped poly(ethylene oxide)–poly(propylene oxide) tetrablock copolymer with SiO_2 nanoparticles for solid-state

supercapacitor applications. ACS Omega 6(26):16924–16933. https://doi.org/10.1021/acsomega.1c01623
46. Li X et al (2021) Recent applications and developments of Polyurethane materials in pavement engineering. Constr Build Mater 304:124639. https://doi.org/10.1016/j.conbuildmat.2021.124639
47. Dhapola PS et al (2024) Environment-friendly approach for synthesis of promising porous carbon: empowering supercapacitors for a sustainable future. Mater Adv 5(6):2430–2440. https://doi.org/10.1039/D3MA00984J

Publisher's Note Springer Nature remains neutral with regard to jurisdictional claims in published maps and institutional affiliations.

Springer Nature or its licensor (e.g. a society or other partner) holds exclusive rights to this article under a publishing agreement with the author(s) or other rightsholder(s); author self-archiving of the accepted manuscript version of this article is solely governed by the terms of such publishing agreement and applicable law.